ELSEVIER

Contents lists available at ScienceDirect

Journal of Environmental Management

journal homepage: www.elsevier.com/locate/jenvman



Research article

Biochar acidification increased sorption and reduced leaching of nitrate

Jannis Grafmüller ^{a,b,*} , Hans-Peter Schmidt ^b, Daniel Kray ^a , Thomas D. Bucheli ^c , Haike Mäurer ^d, Jens Möllmer ^d, Heiko Peisert ^e , Nikolas Hagemann ^{b,c}

- ^a Institute of Sustainable Energy Systems (INES), Offenburg University of Applied Sciences, Germany
- ^b Ithaka Institute, Arbaz, Switzerland and Goldbach, Germany
- ^c Environmental Analytics, Agroscope, Zurich, Switzerland
- ^d Institut für Nichtklassische Chemie e.V. (INC), Leipzig, Germany
- ^e Institute for Physical and Theoretical Chemistry, University of Tuebingen, Tuebingen, Germany

ARTICLE INFO

Keywords: Pyrolysis Protonation Agriculture Plant nutrients biochar acidification Nutrient leaching

ABSTRACT

Biochar can reduce nitrate (NO_3^-) leaching from soil, yet typically only at high, uneconomic application rates. Therefore, biochar should be produced and modified to achieve high sorption capacity. Increased NO_3^- sorption at acidic pH has been reported. However, the sorption mechanisms and potential of biochar acidification to reduce nitrate leaching remain unexplored. Here, NO_3^- sorption was quantified at soil-relevant pH of 5 and 7 on woody biochars produced at highest treatment temperatures (HTT) of $400-900^\circ$ °C. Sorption capacities ranged between 700 and 6200 mg NO_3^- N kg $^{-1}$ at pH 5 and between 200 and 2500 mg NO_3^- N kg $^{-1}$ at pH 7. Thus, NO_3^- sorption to biochar might be higher in acidic compared to neutral soils and can be maximized by producing biochars at HTT \geq 750 °C. Correlation of sorption data with content of surface functional groups and proxies for biochar aromaticity suggest that NO_3^- is sorbed to protonated aromatic structures in biochars produced at $>500^\circ$ C, while NO_3^- might sorb to protonated functional groups in biochar produced at 400° C. Further, biochar acidification under NO_3^- enrichment was tested to reduce NO_3^- leaching. Both in aqueous suspension and in soil columns, full NO_3^- release from KNO_3 -enriched industrial biochar was prevented by biochar acidification, i.e., combined HNO_3+KNO_3 enrichment. In soil with pH 5.7 or pH 7.4, only acidified biochar reduced NO_3^- leaching by up to 23 % and 12 %, respectively, compared to the soil-only control. Thus, acidification could be an interesting approach to produce biochar-based fertilizers with controlled NO_3^- release.

1. Introduction

Nitrogen (N) is often the primary limiting factor for crop production and thus a key component of fertilizers (Schubert, 2018). In mineral fertilizers, N can be added as nitrate (NO_3^-) or, if other N sources are used, soil microbes typically oxidize these to NO_3^- , which is subject to a high risk of leaching to groundwater due to the prevailing negatively charged surfaces of soils (Borchard et al., 2019). This limits the N use efficiency of agriculture.

Biochar is the solid product of biomass pyrolysis and is suggested for use as a soil amendment in agriculture (Lehmann and Joseph, 2015). Biochar reduces NO_3^- leaching by 13 % on a global average (Borchard et al., 2019). Relevant reductions, however, are only obtained for biochar application rates of 10–40 t ha $^{-1}$ (Borchard et al., 2019), which are economically challenging (Bach et al., 2016). Practical and economic applications are usually <2 t ha $^{-1}$ and an effective amount of biochar in soil would only be achieved after several years of repeated input.

Biochar production and modification should therefore be optimized to generate a more effective sorbent for NO_3^- .

Mechanisms for biochar-induced reduction of NO_3^- leaching include the capture of NO_3^- in an organic coating developed through soil ageing or co-composting (Hagemann et al., 2017; Haider et al., 2020) and electrostatic sorption of NO_3^- (Fidel et al., 2018). As composting of biochar is a time-consuming process, more simple modification techniques are required to improve sorption, which is the focus of this study.

So far, NO_3^- sorption to biochar has been reported to be negligible with capacities \ll 200 mg NO_3^- -N kg $^{-1}$ (Gai et al., 2014; Yang et al., 2017). However, the pH during batch experiments was barely controlled and, therefore, sorption was presumably measured at rather alkaline pH, given that biochar usually has a pH in the range of 8–10 (Ippolito et al., 2020). Indeed, biochars exhibit a significantly higher anion exchange capacity (AEC) at pH 5 compared to higher pH (Banik et al., 2018). Likewise, biochars had a limited NO_3^- sorption capacity at pH levels between 7 and 8 (<400 mg NO_3^- -N kg $^{-1}$), but sorption gradually

^{*} Corresponding author. Institute of Sustainable Energy Systems (INES), Offenburg University of Applied Sciences, Germany. E-mail address: jannis.grafmueller@hs-offenburg.de (J. Grafmüller).

increased to $600~mg~NO_3^-N~kg^{-1}$ at pH 6 and was maximized to $1400~mg~NO_3^-N~kg^{-1}$ for a red oak biochar at pH 4.0 (Fidel et al., 2018). By adjusting the pH to 2.7 with citric acid, a rice husk biochar produced at a highest treatment temperature (HTT) of $700~^{\circ}C$ could completely remove NO_3^- from aqueous solution, leading to sorption of $1400~mg~NO_3^-N~kg^{-1}$, while no NO_3^- sorption occurred without addition of acid (pH 9) (Heaney et al., 2020). In line with that, biochar reduced NO_3^- leaching most effectively in soils with a pH < 5.5~(Borchard~et~al., 2019). Despite these consistent results of increased NO_3^- sorption at lower pH, no study has yet elucidated if acidification could be a method to optimize biochar's capacity to reduce NO_3^- leaching. The sorption mechanisms also remain uninvestigated. So far, biochar acidification has only been investigated in the context of phosphorus availability from biochar-based fertilizers (Kopp et al., 2023).

Different mechanisms might be relevant for improved sorption of anions at lower pH, including protonation of acidic functional groups on the biochar surface, protonation via uptake of protons by basic acting moieties, such as $\pi\text{-electrons}$ on basal planes of graphitic structures, or the presence of O- and N-heterocycles that can impact pH-dependent AEC of biochars (Bartolomei et al., 2019; Boehm, 1994; Lawrinenko and Laird, 2015). These mechanisms add (net) positive surface charge to biochars when in contact with acids. Although pH dependent sorption increased for biochars produced at higher HTT (Fidel et al., 2018), it is unknown which of the abovementioned mechanisms dominate pH dependent sorption.

Due to their alkaline nature, biochar capacity to reduce NO_3^- leaching increases over time after soil application, likely as its pH decreases during the equilibration with the surrounding soil pH (Borchard et al., 2019). As the use of biochar-based fertilizers (BBF) has recently gained attention (Melo et al., 2022), simple pre-treatments that improve the NO_3^- sorption, like acidification, are of interest to ensure maximized leaching reduction right after soil application. Any acidified biochar will equilibrate to soil pH with time, determining its long-term pH-dependent sorption capacity. Still, acidification might prevent a rapid leaching of biochar-spiked NO_3^- immediately after soil application.

Here, NO₃ sorption to wood-based biochars produced in an industrial-relevant pyrolysis process at HTT ranging from 400 to 900 °C was studied at soil-relevant pH (pH 5 and 7) along with in-depth biochar characterization, allowing to conclude about the relevance of oxygen containing functional groups and aromaticity of biochars for NO3 sorption. Nitric acid was used for pH control to add no further competitive anions to the experiments aiming to maximize NO₃ sorption, contrasting to earlier studies (Chintala et al., 2013; Fidel et al., 2018; Heaney et al., 2020). The effect of biochar acidification on leaching of NO₃ was studied in soil columns with two contrasting soils. This study aims to (1) improve our understanding of which biochar properties contribute and dominate pH dependent NO₃ sorption and (2) answer the question whether acidification of biochar reduces NO3 leaching from BBF amended soil. We hypothesize that an increase in aromaticity can explain the increased pH dependent NO3 sorption previously reported for biochars produced at increased HTT and that biochar acidification reduces NO₃ leaching from soil.

2. Materials and methods

2.1. Biochar materials

Biochar production was performed with a PYREKA research pyrolysis unit (Pyreg GmbH, Dörth, Germany) using milled and sieved beech wood particles (2<x<6 mm, Verora AG, Edlibach, Switzerland) with a residence time of 10 min at a HTT of 400 °C, 525 °C, 750 °C, and 900 °C. The pyrolysis reactor was electrically heated and is explained in more detail elsewhere (Hagemann et al., 2020). The biochars are referred to as BC400, BC525, BC750, and BC900. Wood was used as it is currently the most widely used feedstock for biochar production across Europe. Industrial wood biochar (BCi) was obtained from AWN GmbH (Buchen,

Germany), who used a Pyreg P500 pyrolysis reactor (Pyreg GmbH) at a HTT of \sim 650 °C and 20 min residence time (PYREG, 2025). The BCi had EBC-Feed certification according to the European biochar Certificate (EBC) under batch reference ba-de-54-1-2 (EBC 2012-2024, 2024). Biochars were milled to <200 μ m with an impact mill (Kinematica AG, Lucerne, Switzerland) and stored in air-tight glass jars at ambient temperature in the dark for further usage. The biochars were characterized according to the methods described in chapter 1 in the Supplementary Information (SI). Where applicable, EBC methods were used (EBC 2012-2024, 2024).

2.2. Batch sorption experiments

Biochars were first conditioned over a total of 12 days to achieve the targeted pH values, i.e., pH 5.0 \pm 0.1 or pH 7.0 \pm 0.1, in a stock suspension (10 stock suspensions in total). To do so, \sim 0.4 g of dry biochar (actual weights were recorded to 0.1 mg accuracy) were weighed into 100 mL Schott bottles and 80 mL of ultrapure water was added. The bottles were placed on a magnet stirrer at room temperature. Over 9 days, the pH value of the suspensions was adjusted by adding diluted HNO3, and the added volumes were recorded. From day 9 onwards, the pH of all stock suspensions was stable. On day 12, all suspensions were quantitatively transferred to a 100 mL graduated cylinder and filled up to the mark using either diluted HNO3 with pH 5 or ultrapure water with pH 7.

For batch sorption experiments, 1.45 mL of the stock suspensions were aliquoted under constant stirring at 700 rpm into 2 mL polypropylene reaction vessels. A volume of 0.05 mL of five different KNO₃ solutions was pipetted to each reaction vessel to add additional 0, 10, 20, 50, 100, or 240 mg NO₃-N L⁻¹ to the suspension besides already contained NO₃ originating from HNO₃ in the stock suspension (Table S1). The resulting biochar concentration in each reaction vessel was 4 g L⁻¹. Establishment of equilibrium phase distribution was assured by initially following adsorption kinetics with 100 mg NO₃-N L^{-1} added to the suspensions in triplicates for either 1, 3, 6, 16, 24, or 48 h. For all other added NO₃ concentrations, equilibration was done for only 48 h. The reaction vessels were equilibrated horizontally fixed on a rotary shaker at 220 rpm and 25 $^{\circ}\text{C}$ (KS 4000 ic control, IKA Werke GmbH&Co. KG, Staufen, Germany). Samples equilibrated for 48 h with either 20 or 100 mg NO_3^- -N L^{-1} were centrifuged after equilibration with 17,000×g at 25 °C (Fresco™ 17, Thermo Fisher Scientific, Waltham, USA), to obtain a biochar pellet for later NO₃ desorption experiments (Fig. S1). The supernatants or suspensions, if not centrifuged, were filtered (<0.45 µm, Nylon, Chrompure, Membrane-Solutions LLC, Auburn (WA), USA) and filtrates were stored at −18 °C for later NO₃ analysis.

2.3. Nitrate desorption from biochar

After centrifugation (cf. Section 2.2, Fig. S1), biochar pellets were resuspended in 1.5 mL of either diluted HNO₃ adjusted to pH 5 (for samples previously equilibrated at pH 5) or ultrapure water with pH 7 (for samples previously equilibrated at pH 7). Samples were equilibrated for 48 h and subsequently centrifuged and filtered as described above. A second desorption step was performed in the same way. Additional triplicate samples equilibrated in previous sorption experiments for 48 h with added 100 mg NO $_3$ -N L $^{-1}$ were used for desorption experiments as described above, but desorption was performed in 1 M KCl and only in a single step for 48 h. Before the first and second desorption steps, the reaction vessels including the biochar pellet were weighed to estimate the remaining non-decanted liquid volume to correct for already solubilized/desorbed NO $_3$ -.

2.4. Experiments with BBF

2.4.1. BBF preparation

Two different BBF were prepared from BCi. The BCi was weighed into 50 mL centrifuge tubes and moistened with two different NO_3^- solutions to 80 % of its WHC (=230 %, w/w), which equaled 1.83 mL g $^{-1}$. For release experiments (cf. Section 2.4.2), 0.4 g, and for column leaching experiments (cf. Section 2.4.3), 0.09 g of dry matter equivalent of BCi was used. The first solution contained only KNO $_3$ at 138 g L $^{-1}$, the BBF enriched with this solution was termed BCi-N. The second solution contained a mixture of HNO $_3$ (27.4 mL concentrated HNO $_3$ L $^{-1}$) and KNO $_3$ (95 g L $^{-1}$), in which 31 % of total NO $_3^-$ originated from HNO $_3$. The BBF prepared with this solution was labeled as BCi-HNO $_3$. Each solution was pipetted onto the whole surface of the biochar, vortexed after 2 h, and left to stand for 3 days at room temperature. Both BBFs were enriched to a calculated NO $_3^-$ content of 3.5 % N (w/w). After enrichment, BCi-N had a pH value of 9.0 and BCi-HNO $_3$ of 5.4.

2.4.2. Nitrate release from BBF

Nitrate release from BCi-N and BCi-HNO₃ was measured in triplicates in a 0.5 M phosphate buffer either adjusted to pH 5.7 or pH 7.4. The buffers were prepared from a stock solution of KH₂PO₄ and Na₂HPO₄ x 2H₂O. A buffer volume of 20 mL was added to the centrifuge tube with the prepared BBF (cf. section 2.4.1), and samples were horizontally shaken at 150 rpm and room temperature. Four sequential desorption steps of each 48 h were performed. After each desorption step, samples were centrifuged at 10,000×g for 5 min (Megafuge 16, Thermo Fisher Scientific, Waltham, USA) and 15 mL of the supernatant were exchanged with fresh buffer while filtering a subsample of the supernatant through a syringe filter for storage at -18 °C. For N release monitoring during the first desorption step, samples were centrifuged as described above after 1, 3, 8, and 24 h and 0.5 mL of the supernatant was sampled. Fresh 0.5 mL buffer were added to maintain a constant solid to liquid ratio. Total released N from the BBF into the buffer after each desorption step $(R_{N,i})$ in % (w/w) was calculated with equation (2) given in section 1.6 in the

2.4.3. Nitrate leaching from BBF amended soil columns

Two different standard soils were used in the experiment, which are referred to as "soil-2.3" with pH 5.7 (silt sand) and "soil-2.4 N" with pH 7.4 (normal loam) according to the soil provider (LUFA, Speyer, Germany, for soil characteristics see Table S2). Columns were prepared by mixing 12 g dry matter of soil and biochar added via BCi-N or BCi-HNO₃ (0.75 % biochar concentration, w/w). A fertilized treatment without biochar was also included (Control), here a NO₃ solution adding 3 mg N per column, as with BCi-N and BCi-HNO3, was applied. The spiked Control soil was left to stand for 3 days in 50 mL centrifuge tubes (similar as BCi-N and BCi-HNO3, cf. Section 2.4.1) before the soil was homogenized and packed into the columns. BCi-N and BCi-HNO3 were homogeneously mixed with the soil and packed into columns. The columns were 10 mL polypropylene syringes and contained a 0.15 g glass wool layer at the bottom. Non-fertilized controls with or without BCi were also included. The water holding capacity (WHC) of each soil mixture was measured by submersion of the whole column in water for 24 h with a subsequent drainage of 2 h. The total H₂O remaining in the soil column after drainage was defined as 100 % WHC or one soil pore volume (SPV, corrected for contributions from syringe and glass wool). These soil columns for WHC measurement were prepared in addition and not used for later leaching experiments.

The columns were watered to 65 % WHC for three days and then to 95 % WHC on the fourth day after setup. On day 4, 7, 8, and 9, water was added on top of the columns, 2.3 mL for treatments with soil-2.3 and 2.98 mL for soil-2.4 N, both equal to 0.5 SPV (Fig. S2). Ultrapure water was used in all steps. Leachates were filtered and stored as described above. On day 12, 150 μ l of a 144 g L⁻¹ KNO₃ solution were pipetted on top of the column for re-fertilization with 3 mg NO₃-N. Further leaching

events were conducted on day 14, 15, 16, 17, and 18 as described above.

2.5. Nitrate quantification

 NO_3^- concentrations in filtrates were measured in 96-well microplates and a microplate reader (Biotek Epoch 2, Agilent Technologies Inc., Santa Clara, USA) (Hood-Nowotny et al., 2010). A Thermomixer C (Eppendorf SE, Hamburg, Germany) was used for plate incubation for 1 h at 37 $^{\circ}$ C and the calibration curve was recorded in a range of 0–2.5 mg NO_3^- -N L $^{-1}$ with KNO $_3$ as standard. All reagents were of analytical grade and either purchased from Carl Roth GmbH & Co. KG (Karlsruhe, Germany) or Merck KGaA (Darmstadt, Germany).

2.6. Data analysis

Calculation of sorbed amounts of NO_3^- on biochars in batch sorption experiments (c_s in mg NO_3^- -N kg $^{-1}$) and their fitting to the Freundlich and Langmuir model are described in section 1.7 of the SI. The sorption capacities obtained from the Langmuir model ($c_{s,max}$) were normalized to different biochar properties according to section 1.8 in the SI to identify potential sorption mechanisms.

Data from release and column experiment was analyzed by an unpaired t-test at $\alpha < 0.05$ by either comparing BCi-HNO $_3$ with BCi-N (release experiment) or BCi-HNO $_3$ and BCi-N individually with the Control (column experiment), respectively, for each desorption or leaching step. Data normality and variance homogeneity were evaluated with a Shapiro-Wilk test and a Brown-Forsythe test, respectively. Data visualization and analysis was performed with GraphPad Prism (version 10.0.3, Graphpad Software LLC, Boston, USA).

3. Results

3.1. Chemical properties of biochars

The C and ash content, as well as pH of the biochars, increased with HTT (Table 1). By increasing HTT from 400 °C to 525 °C, SEC increased by four orders in magnitude and ultimately rose to 1.4·10³ mS cm⁻¹ and 1.3·10⁴ mS cm⁻¹ for a HTT of 750 °C and 900 °C, respectively, indicating higher aromaticity of biochars produced at higher HTT, in line with a reduction in hydrogen to organic carbon molar ratio (H/C_{org}, Table 1). Boehm titration indicated a decrease in the amount of acidic functional groups, i.e., total acidity of the biochars, with increasing HTT from 0.58 mmol g⁻¹ (BC400) to 0.08–0.22 mmol g⁻¹ (BC525-BC900, Table 1), but carboxylic groups were still detected for BC750 and BC900 (Fig. S3). In contrast, the amount of basic functional groups increased with HTT (Table 1). Spectroscopic analyses delivered evidence for decreased oxygen-containing functional group contents on the biochars produced at higher HTTs. The FTIR spectrums revealed a loss of H-bonded OHgroups (3400-3200 cm⁻¹), a decrease in phenolic OH bending at 1390 cm⁻¹ and a general loss of characteristic carboxylic group bands e. g., the C=O stretching band at 1690 cm⁻¹ (from carboxylic acids or esters), the COO^- band at $\sim 1580~{\rm cm}^{-1}$ and carboxylic C-OH band at $\sim\!1200~\text{cm}^{-1}$ with increasing HTT (Fig. 1). The FTIR-band pattern of BCi was closely related to that of BC525 (Fig. 1). The XPS-derived surface O/ C molar ratio decreased with an increase in HTT (Table 1 and Table S3) and the appearance of high binding energy satellite structures at around 291 eV may indicate an increase of aromaticity for BC750 and BC900 (Fig. S4). The SSA of biochars based on N₂ sorption increased drastically with HTT from 6 to 388 m² g⁻¹ while SSA based on CO₂ sorption was generally higher (Table 1), indicating limited accessibility for N2 at the applied measurement conditions (-195.8 $^{\circ}\text{C}$ at 0.1 MPa), especially to the pore system in BC400. The SSA of pores with a diameter >0.67 nm, i. e., the range of pores most relevant for NO₃ sorption due to the diameter of hydrated NO₃ of 0.67 nm (Nightingale, 1959), were in a narrow range across biochars (42-59 m² g⁻¹), only BC525 had a SSA theoretically accessible for NO₃ of only 28 m² g⁻¹ (Table 1 and Fig. S7).

Table 1

Elemental analysis (carbon – C, organic carbon - C_{org} , hydrogen – H, nitrogen – N in % (w/w) and molar H/ C_{org} ratio), ash content (w/w), pH, solid-state electric conductivity (SEC), surface molar O/C ratio (derived from X-ray photoelectron spectroscopy), total acidity and total basicity obtained from Boehm titration, as well as cumulative specific surface area (SSA) based on CO_2 and N_2 gas adsorption calculated with the Brunauer-Emmett-Teller model (CO_2 - and N_2 -SSA). The CO_2 -SSA is also presented covering only pores with a width of >0.67 nm. The beech-wood biochars were produced at a highest treatment temperature of 400, 525, 750, and 900 °C (BC400, BC525, BC750 and BC900, respectively) and the industrial wood-based biochar at ~650 °C (BCi). n.d.: not determined. All analyzes were performed without repetitions, except the ash content and total acidity, which were performed as triplicate measurements.

	C [%]	C _{org} [%]	H [%]	N [%]	H/ C _{org}	Ash [%]	pН	SEC [mS cm ⁻¹]	Surface O	,	Total acidity [mmol g ⁻¹]	Total basicity $[mmol g^{-1}]$	$\begin{array}{c} \text{CO}_2\text{-SSA }[\text{m}^2\\ \text{g}^{-1}] \end{array}$	CO_2 -SSA (>0.67 nm) $[m^2 g^{-1}]$	N_2 -SSA $[m^2$ $g^{-1}]$
BC400	78.0	77.7	3.8	0.5	0.58	3.1 ± 0.1	6.9 9.6	$6 \cdot 10^{-7}$	0.16	(0.58 ± 0.01	0.16	241	50	6
BC525	87.0	86.7	3.2	0.8	0.44	3.3 ± 0.2	9.1 9.3	3.10^{-3}	0.12	(0.08 ± 0.01	0.31	347	28	249
BC750	91.1	90.3	1.5	0.8	0.20	4.5 ± 0.1	9.4 1.4	4.10^{3}	0.11	(0.22 ± 0.01	0.79	410	42	372
BC900	91.4	90.8	1.5	0.9	0.20	4.9 ± 0.1	9.7 1.3	3.10^{4}	0.09	(0.22 ± 0.01	0.91	465	50	388
BCi	89.1	88.8	1.7	0.6	0.23	5.2	8.6 1.7	7·10°	n.d.	I	n.d.	n.d.	388	59	9

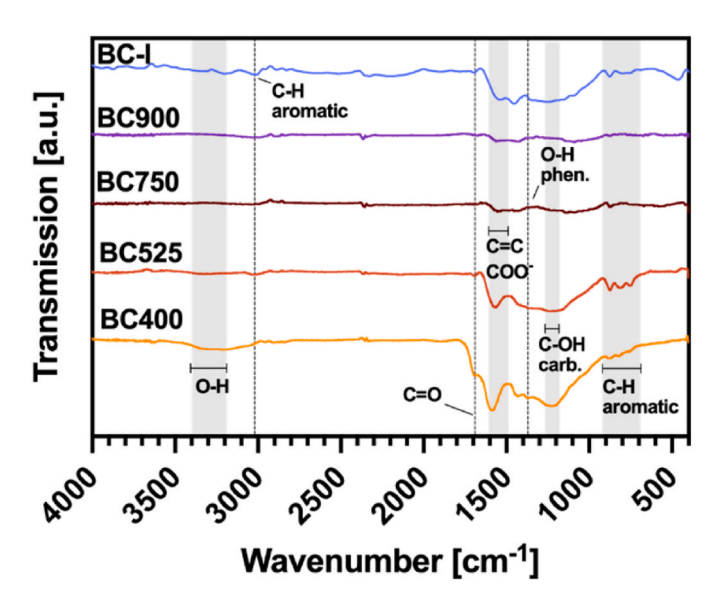


Fig. 1. (A) Baseline-corrected Fourier-Transform Infrared (FTIR) spectrums of beech-wood biochars produced at pilot-plant scale at 400, 525, 750 and 900 °C (BC400, BC525, BC750 and BC900, respectively), and of industrial wood-based biochar (BCi, produced at \sim 650 °C). Band allocation was done according to literature (Singh et al., 2017). a.u.: arbitrary unit.

3.2. Nitrate sorption isotherms

Equilibrium water-biochar phase distribution of NO₃ was stable after 48 h in preliminary tests for all biochars at both pH values (Fig. S8). Fig. 2 presents the calculated sorbed amount of NO₃ on the different biochars over the c_w value and the fitted sorption models. The goodness of fit, i.e., R² values, were similar for the Langmuir and Freundlich sorption models (Table 2). Sorption was higher at pH 5 compared to pH 7 for all biochars (Fig. 2). At pH 5, NO₃ Langmuir sorption capacities c_s. max, derived from adsorption data only, ranged between 650 mg NO₃-N kg^{-1} (BC400) and 6190 mg $NO_3^-N\ kg^{-1}$ (BC750), while at pH 7, $c_{s,\text{max}}$ varied between only 180 mg NO₃-N kg⁻¹ (BC400) and 2480 mg NO₃-N kg^{-1} (BC900, Fig. 2 and Table 2). For BC750 and BC900, $c_{s,max}$ was in a similar range at pH 5 and it generally decreased in the following order: BC750 > BC900 > BCi > BC525 > BC400 at pH 5 and BC900 > BC750 >BCi > BC525 > BC400 at pH 7. The Freundlich exponent (1/n) was <1for all biochars at all pH values, indicating favorable sorption (Table 2). Freundlich sorption coefficients K_F ranged between 450 and 2740 l kg⁻¹ at pH 5 and between 150 and 2030 l kg⁻¹ at pH 7 and decreased in the following order: BC900 > BCi > BC750 > BC525 > BC400 at pH 5 and BC900 > BC750 > BCi > BC525 > BC400 at pH 7.

There was a good positive linear correlation of $c_{s,max}$ with the CO₂-based SSA (R² = 0.83–0.98, Fig. 3a), but no correlation was observed with CO₂-based SSA actually available for NO₃ sorption (Fig. 3b), i.e.,

SSA contributed by pore widths >0.67 nm, which corresponds to the hydrated diameter of NO_3^- (Nightingale, 1959). High positive correlation was also observed with the decadic logarithm of SEC and the total basicity of the biochars (Fig. 3a–c and d). The $c_{s,max}$ was negatively correlated with the molar H/C_{org} ratio and molar surface O/C ratio of biochars, but for the latter with lower goodness of fit, especially for sorption data obtained at pH 5 (Fig. 3e and f). There was no clear trend observable between $c_{s,max}$ and total acidity quantified by Boehm titration (Fig. S11).

Normalization of $c_{s,max}$ to available CO₂-based SSA (pore widths >0.67 nm) illustrated that monolayer sorption dominated at pH 7 while at pH 5, multilayer sorption was indicated for BC750 and BC900 (Fig. S9a). Normalization of $c_{s,max}$ to total basicity reduced variation between different biochars to 23 % at pH 5 and 36 % at pH 7 (Fig. S9c), which is considerably lower compared to variation of non-normalized values for $c_{s,max}$ (59 % at pH 5 and 54 % at pH 7).

Desorption experiments indicated hysteresis for BC525, BCi and BC900 at pH 5 and for BC525, BCi and BC750 at pH 7 (data points filled in white, outlined in color, Fig. 2).

3.3. Release of NO₃ from BCi-N and BCi-HNO₃

Release of NO₃ from two different BBF (BCi-N and BCi-HNO₃) was studied in a 0.5 M phosphate buffer, adjusted to pH 5.7 or 7.4, similar to the pH values of the soils used in the column leaching experiment (cf. Section 3.4). In the first desorption step, BCi-N and BCi-HNO3 released respective 85 % and 81 % of NO_3^- at pH 5.7 (p = 0.25, Table S4), while respective 92 % and 83 % (p = 0.06, Table S4) were desorbed at pH 7.4 (Fig. 4a and c). All samples released an additional 3-4 % NO₃ during the second desorption step, regardless of buffer pH. After four desorption steps, cumulative release from BCi-N and BCi-HNO3 stabilized at respective 88 % and 85 % for pH 5.7 (p = 0.33) and at 96 % and 90 % at pH 7.4 (p = 0.10). After the fourth desorption step, respective 3.9 and 4.8 g NO₃-N kg⁻¹ remained sorbed in BCi-N and BCi-HNO₃ at pH 5.7 (p > 0.05, Table S4), while 2.2 and 3.5 g $NO_3^-N~kg^{-1}$ (p > 0.05), respectively, remained sorbed at pH 7.4. Initially, 35 g NO₃-N kg⁻¹ were added to the biochar. Most NO₃ was already desorbed after 1 h from all BBF during the first desorption step (Fig. 4 b and d, Table S5).

3.4. Nitrate leaching from soil amended with BCi-N and BCi-HNO₃

Amending BCi-HNO $_3$ to soil-2.3 with pH 5.7 significantly reduced cumulative NO $_3$ leaching in the first four leaching events by 23 %, 13 %, 9 % and 8 %, respectively, compared to the Control (p < 0.05), which was not observed with BCi-N (Fig. 5a and c). Amendment of BCi-N resulted in a higher deviation between the three replicates (coefficient of variation - CV = 9 %) than observed both for the Control (CV = 2 %) and soil amended with BCi-HNO $_3$ (CV = 4 %). In soil-2.4 N with pH 7.4, BCi-HNO $_3$ significantly reduced cumulative NO $_3$ leaching by 12 % compared to the Control after 0.5 SPV (p < 0.05) and by 16 % when correcting for native NO $_3$ leached from the soil, but there was no

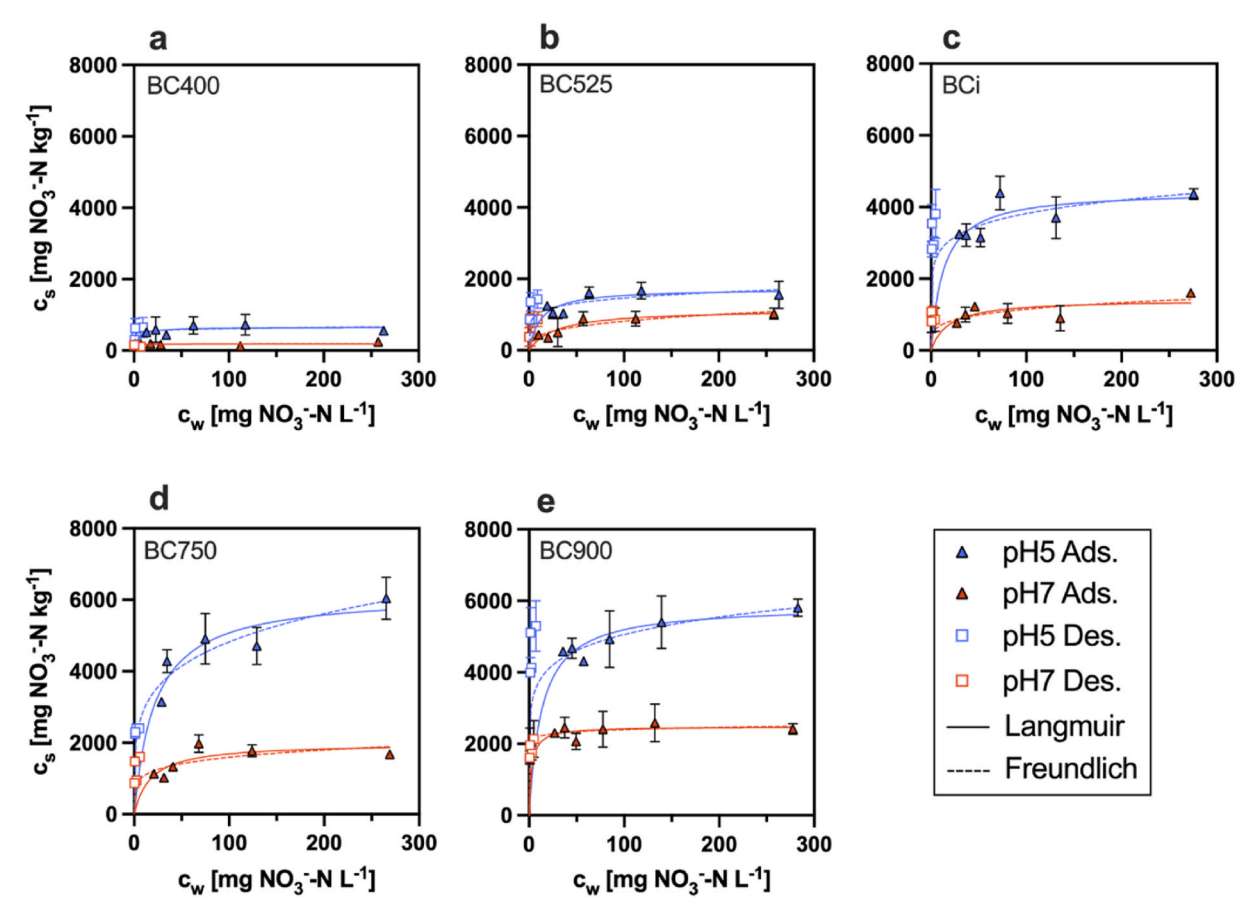


Fig. 2. Nitrate sorption isotherms of four wood-based biochars produced at pilot plant scale at 400, 525, 750, and 900 °C (BC400, BC525, BC750, and BC900 in panels a, b, d, and e, respectively) and at industrial scale (BCi, \sim 650 °C, panel c). Sorption was studied at pH 5.0 and 7.0 by equilibration in triplicates at 25 °C for 48 h. Filled data points represent the adsorption (Ads.) and white, color-bordered data points represent the desorption branch (Des.). c_s : calculated nitrate-nitrogen (NO $_3$ -N) concentration in the solid phase (= sorbed on biochar). c_w : NO $_3$ -N concentration in liquid phase. Error bars indicate the standard deviation. Solid and dashed lines represent the fitted Langmuir and Freundlich sorption models, respectively. Fitting parameters are presented in Table 2.

Table 2 Fitting parameters and correlation coefficients of the Langmuir and Freundlich models (cf. equations (4) and (5) in section 1.7 in the Supplementary Information) for nitrate-nitrogen (NO_3 -N) sorption onto biochars produced at pilotplant scale at 400, 525, 750, and 900 °C (BC400, BC525, BC750, and BC900, respectively) and at industrial scale (BCi, produced at \sim 650 °C). Sorption experiments were conducted at pH 5.0 and 7.0 with equilibration at 25 °C for 48 h.

Biochar	Lang	muir		Freundlich		
	$c_{s,max}$ [mg NO $_3^-$ -N kg $^{-1}$]	$K_{\rm L}$ [L kg $^{-1}$]	R ²	1/n	${ m K_F}$ [L ${ m kg}^{-1}$]	R ²
pH 5.0						
BC400	650	0.240	0.87	0.067	450	0.86
BC525	1720	0.082	0.92	0.151	730	0.90
BC750	6190	0.046	0.96	0.219	1760	0.96
BC900	5880	0.076	0.98	0.133	2740	0.99
BCi	4450	0.078	0.95	0.135	2050	0.94
pH 7.0						
BC400	180	2.140	0.78	0.047	150	0.79
BC525	1140	0.034	0.93	0.305	200	0.91
BC750	1980	0.057	0.90	0.173	720	0.85
BC900	2480	0.385	0.97	0.036	2030	0.97
BCi	1420	0.054	0.82	0.216	430	0.85

significant difference compared to the Control in cumulative NO_3^- loss after 1.0, 1.5, and 2.0 SPV leached through the columns (Fig. 5b and d). With fertilization, almost all initial NO_3^- applied to the columns (3 mg NO_3^- -N) either by direct soil fertilization or via BCi-N and BCi-HNO $_3$ was released after leaching both soils with 2 SPV. For non-fertilized soil,

0.2–0.3 mg NO_3^- -N were leached from soil-2.3 and 1.3 mg NO_3^- -N were released from soil-2.4 N after 2 SPV, independent of a biochar amendment (Fig. 5a and b).

After re-fertilizing the columns by applying a fertilizer solution on top of the soil surface, BCi-HNO $_3$ significantly reduced cumulative leaching compared to the control by 15 % at 2.5 SPV, by 22 % at 3.0 SPV and by almost significant 10 % after 3.5 SPV (p = 0.0534) in soil-2.3 (Fig. 5a and c). BCi-N only reduced cumulative leaching significantly after 3.0 SPV by 10 % compared to the control (Fig. 5a and c). In soil-2.4 N, both BCi-N and BCi-HNO $_3$ significantly reduced cumulative leaching after 3 SPV by 7 % and BCi-HNO $_3$ further reduced it by 7 % after 3.5 SPV (Fig. 5b and d). In the following, no significant differences in cumulative N leaching were observed.

4. Discussion

4.1. NO_3^- sorption and desorption at soil-relevant pH

For all biochars, the decrease from pH 7 to pH 5 increased NO_3^- sorption capacities by a factor of 1.5–3.6 (average = 2.8). The increase in sorption capacity with a reduction in pH can be explained by biochar surface protonation under acidic conditions, which increases the net positive surface charge (Lawrinenko and Laird, 2015). As normalization of $c_{s,max}$ related to SSA accessible for hydrated NO_3^- ions, i.e., to pores with a width of >0.67 nm (Nightingale, 1959), did not level out differences between individual biochars, it can be concluded that higher sorption with higher HTT was less related to an increase in SSA, but

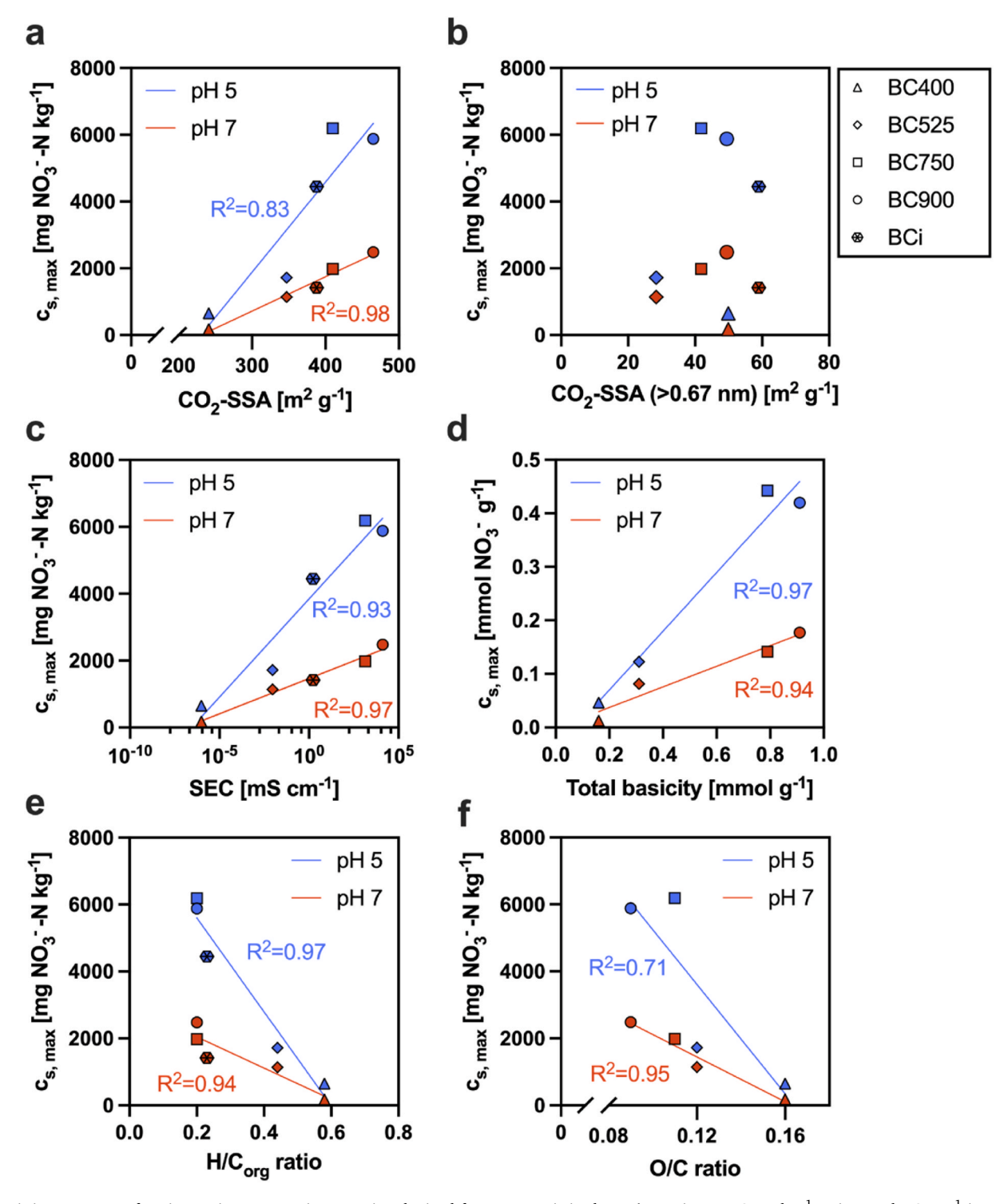


Fig. 3. Fitting parameter for nitrate-nitrogen sorption capacity obtained from Langmuir isotherm ($c_{s,max}$ in mg NO $_3$ -N kg $^{-1}$ or in mmol NO $_3$ g $^{-1}$ in panel d) of biochars plotted over biochar properties: specific surface area (SSA) derived from CO $_2$ sorption (total SSA and SSA contributed by pores >0.67 nm, panels a and b, respectively), solid state electric conductivity (SEC, logarithmic x-axis, panel c), total basicity (panel d), hydrogen/organic carbon molar ratio (H/C $_{org}$), and molar surface oxygen/carbon (O/C) ratio on the biochar surface derived from X-ray photoelectron spectroscopy (panel f). Correlation coefficients, where applicable, are related to linear regressions of the data each for $c_{s,max}$ recorded at pH 5 or pH 7.

rather to other biochar properties.

Oxygen-containing, deprotonated acidic functional groups on the biochar surface can take up protons, representing a partially positively charged sorption site for NO_3^- (Fidel et al., 2018). Boehm titration indicated that the overall acidity of biochars decreased with HTT, in line with the consensus that O-containing functional groups on biochar surfaces are degraded with increasing HTT (Banik et al., 2018).

However, a higher content of carboxylic groups was found for biochars produced at an HTT of 750 $^{\circ}$ C and 900 $^{\circ}$ C, which is not in line with literature (Gezahegn et al., 2019). This finding might be related to methodological biases in Boehm titration, which involves several pre-treatment steps that include acid-washing of biochar samples (Fidel et al., 2013). Residual acid might have been falsely detected as carboxylic groups for these biochars. Despite this, total acidity obtained

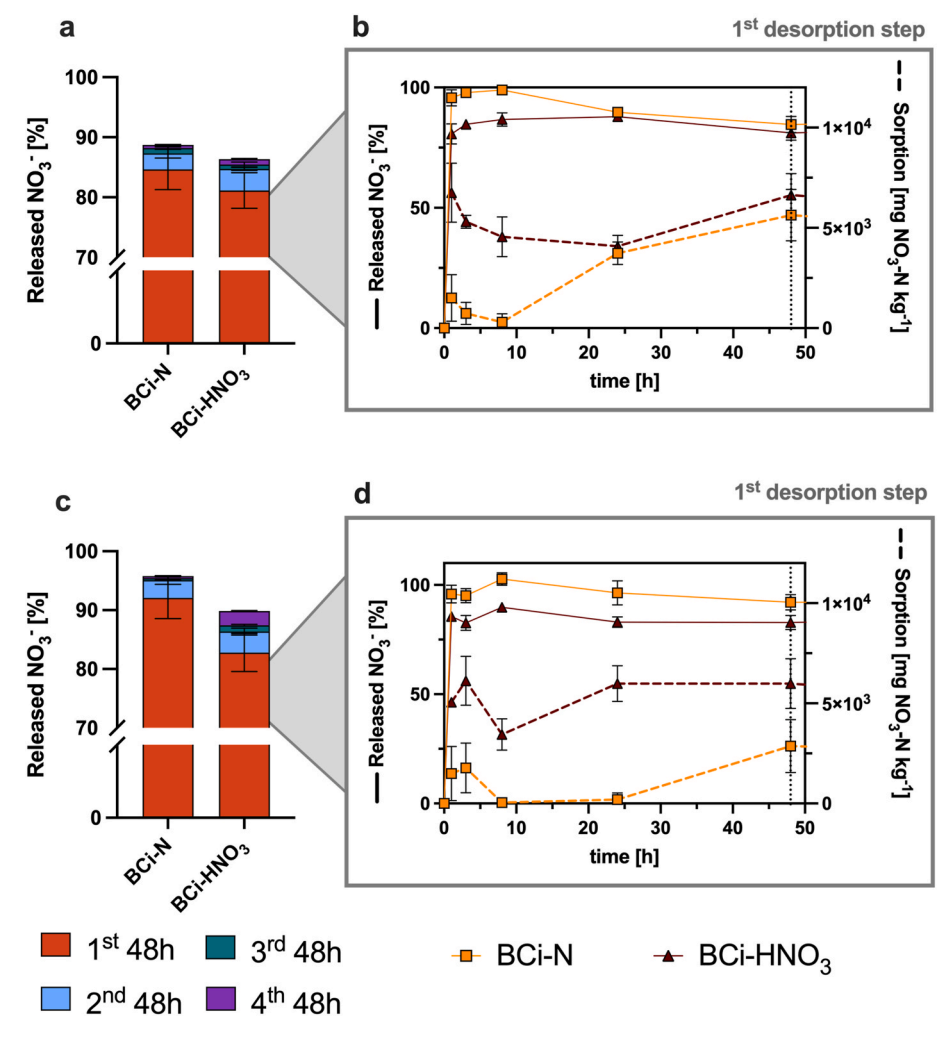


Fig. 4. Released nitrate (NO_3^-) from biochar produced at industrial scale, either enriched with HNO₃ and KNO₃ (BCi-HNO₃) or with only KNO₃ (BCi-N) to a N content of 3.5 % (w/w). Release experiments were performed either in a 0.5 M phosphate buffer adjusted to pH 5.7 (a, b) or to pH 7.4 (c, d) at 1:50 solid to liquid ratio and with shaking at 150 rpm. Panels a and c show the cumulative NO_3^- release during four desorption steps of each 48 h in fresh buffer (note the change in the y-axis scale at > 70 %). Panels b and d present the NO_3^- release (left axis, solid line) and the calculated mass of NO_3^- remaining sorbed onto biochar (right axis, expressed as NO_3^- -nitrogen, NO_3^- -N, dashed line) as a function of time during the first desorption step of 48 h. Error bars indicate the standard deviation of n=3 replicates.

from Boehm titration as well as XPS and FTIR measurements coherently indicate a loss of the total O-containing functional group content with an increase in HTT. Therefore, the increased sorption of NO3 with decreasing pH and increasing HTT may have been less related to protonation of O-containing functional groups. Yet, it may be that NO3 sorption to BC400 was due to this mechanism, as molar-based sorption capacities ranged between 0.01 and 0.05 mmol $NO_3^-\ g^{-1}$, which is well below the quantified acidity of BC400 (0.5 mmol g⁻¹ due to protonated phenols and lactols at pH 7 and 0.58 mmol g⁻¹ by further contribution of protonated carboxylic groups at pH 5). However, for biochars with higher HTT, the observed sorption capacities of up to 0.4 mmol NO₃ g⁻¹cannot be attributed solely to the phenolic group content (0.05 mmol g⁻¹, Fig. S3) and potentially falsely detected carboxyl group content (0.15 mmol g⁻¹), which would anyway have only been present in the relevant protonated form during sorption experiments at pH 5, given their pK_a value of 6.4 (Fidel et al., 2013).

Protons may also be adsorbed on biochars by basic acting groups. Pyrone-like structures have basic character (Boehm, 2001), but since O/C ratios steadily decreased with higher HTT, it is unlikely that these contributed to the increased basicity at higher HTT. Sorption of protons can also occur on delocalized π -systems on the basal planes of graphitic structures (Boehm, 2001). With a higher HTT, graphitization of biochar is increased (Chia et al., 2015), which could explain their higher

basicity, leading to a higher degree of protonation and thus, higher NO₃ sorption at lower pH. Further, SEC of biochars increases with aromaticity and graphitization of biochar (Issi, 2001; Mochidzuki et al., 2003) while molar H/Corg is reduced. The high goodness of fit for the correlation of NO₃ sorption capacities with total basicity, SEC and H/C_{org} ratios (Fig. 3) indicates that sorption of NO₃ on protonated, aromatic structures was likely the main sorption mechanism, especially for biochars produced at HTT >500 °C. This was also indicated by the lowest variation between different biochars upon normalization of $c_{s,max}$ to total basicity (Fig. S9), and is corroborated by lower molar $c_{s,max}$ values compared to the quantified basicity of all biochars (Fig. 3d). Still, it has to be mentioned that there is no validated method available for Boehm titration for biochar basicity as compared to quantification of acidity. Thus, the total basicity measurements might not only cover the uptake of H⁺ by graphitic structures but also a neutralization of ash fractions. Still, while variation in ash content of the different biochars was only 19 %, total basicity varied by 58 % and was thus not dominated by the ash content.

The increase in NO_3^- sorption of biochars under acidic conditions and with HTT aligns with literature on pH-dependent NO_3^- sorption (Chintala et al., 2013; Fidel et al., 2018) and anion exchange capacities of biochars (Lawrinenko and Laird, 2015). The latter reported NO_3^- sorption capacities in a similar range as the present study: 1700–2000

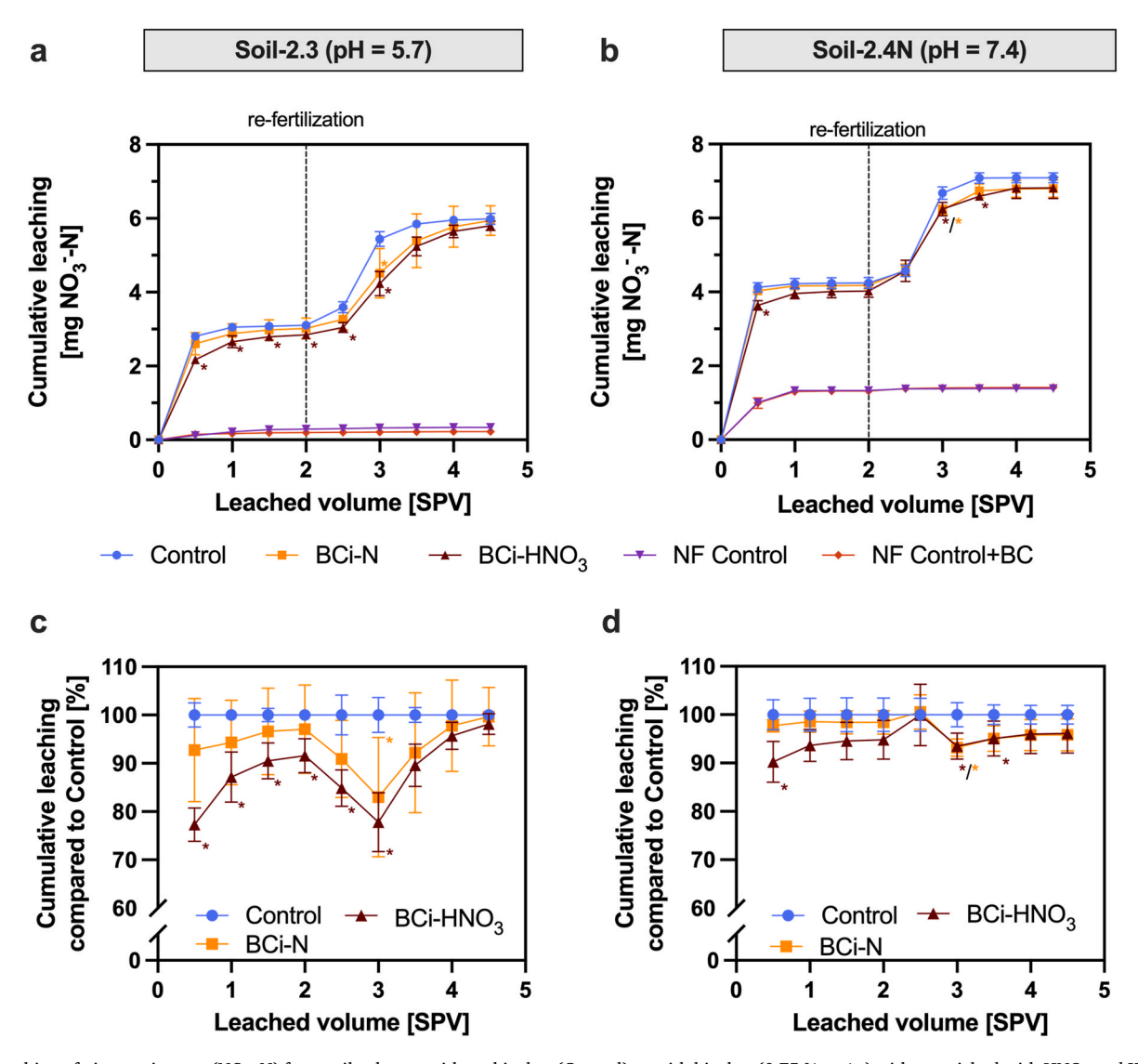


Fig. 5. Leaching of nitrate-nitrogen (NO_3^-N) from soil columns without biochar (Control) or with biochar (0.75 %, w/w), either enriched with HNO_3 and KNO_3 (BCi-HNO₃, bulk pH = 5.4) or with only KNO_3 (BCi-N, bulk pH = 9) plotted over cumulative leachate volume expressed as soil pore volume (SPV). Initial fertilization was 3 mg NO_3^-N via direct soil fertilization or via enriched biochars. Re-fertilization occurred after four leaching events (=2 SPV) with 3 mg NO_3^-N via KNO_3^-N via $KNO_$

mg NO_3^-N kg⁻¹ for corn stover and red oak biochars at pH 3.7 (Fidel et al., 2018) as well as 700–6000 mg NO_3^-N kg⁻¹ at pH 5.0 and 560–4000 mg NO_3^-N kg⁻¹ at pH 7.0 for corn stover, pine wood, and switchgrass biochars (Chintala et al., 2013). This underscores that the type of acid and biochar production methods in the different studies were less influential for NO_3^- sorption capacities as compared to pH values during sorption experiments and HTT. In the light of the present study, the absent NO_3^- sorption capacities discovered by Gai et al. were likely due to a lack of pH control and resulting alkaline conditions (Gai et al., 2014).

As HNO $_3$ was used for pH control in our experiments, low equilibrium concentrations below $10\text{--}30~\text{mg}~\text{NO}_3^-\text{-N}~\text{l}^{-1}$ could not be covered in the sorption experiments. Therefore, sorption in this range cannot be described with sufficient certainty by our models. Still, this does not significantly affect the extent of the Langmuir sorption capacity $c_{s,max}$ derived from our model, which is the focus of our sorption experiment. The full release during desorption in 1 M KCl with average NO_3^- recovery rates of 80--115~% indicated a closed mass balance in the sorption-

desorption experimental series (Fig. S10).

4.2. NO₃ release from BCi-N and BCi-HNO₃ in phosphate buffer

Biochar-based fertilizers were produced by enriching biochar with 35 g NO $_3$ -N kg $^{-1}$, i.e., a significantly higher amount of N compared to the maximum sorption capacity of BCi (4.5 g NO $_3$ -N kg $^{-1}$, Table 2). The acidification of biochar significantly reduced NO $_3$ release during the initial hours of the first desorption step at both pH values (pH 5.7 and pH 7.4, Table S5), but differences between non-acidified and acidified BBF were generally small. Desorption of 80–90 % of applied N from all BBF in general occurred fast, i.e., within the first hour of desorption.

BCi-N demonstrated re-sorption of previously released NO_3^- during the first desorption step, with this effect being more pronounced at pH 5.7 than at pH 7.4. The initial pH of BCi-N was 9.0, and during the release experiment, BCi-N equilibrated to the pH of the buffers, which in turn increased its NO_3^- sorption capacity. This explains the alignment in residual sorbed and released NO_3^- of BCi-HNO₃ and BCi-N after 24 h

during the first two desorption steps at pH 5.7, when equilibration seemed complete. At pH 7.4, the differences in NO_3^- release between BCi-N and BCi-HNO $_3$ persisted for a longer period, i.e., until the third desorption step was finished. At higher environmental pH levels, biochar acidification could therefore improve NO_3^- sorption to biochar over a longer period than at lower pH.

The results generally imply that acidifying biochar can reduce the NO_3^- release from NO_3^- -enriched biochar, particularly in the short term after soil application. During this phase, the sorption capacity of pristine biochar may still be limited due to its alkalinity and delayed equilibration to soil pH. In contrast, acidified biochar exhibits a higher initial affinity for NO_3^- immediately upon application. In the long term, however, both acidified and non-acidified biochar will equilibrate to the surrounding soil pH, eliminating the effects of the acidification treatment, as observed in the release experiments, and both biochars would undergo ageing in soil contributing to NO_3^- capture in biochar (Hagemann et al., 2017; Haider et al., 2020).

The release dynamic of NO_3^- from biochar pores is not only regulated by NO_3^- sorption to the biochar surface, but also by mobility of water molecules inside biochar pores that hydrate NO_3^- ions (Conte and Schmidt, 2017). Both processes overlapped in the extraction experiment and can therefore not be differentiated. The effect of biochar acidification on water mobility within biochar pores could e.g., be separately studied by Fast-Field Cycling Nuclear Magnetic Resonance Relaxometry (Conte and Schmidt, 2017).

In general, the non-released NO_3^- after the release experiment for BCi-N was 4.5 g NO_3^- -N kg⁻¹ at pH 5.7 (13 % of initial N enrichment) and 1.4 g NO_3^- -N kg⁻¹ at pH 7.4 (4 % of initial N enrichment), which aligns with $c_{s,max}$ values calculated for BCi based on the batch sorption experiments (Table 2).

4.3. NO₃ leaching in soil column experiment

In the first leaching event, NO₃ leaching was significantly reduced only with BCi-HNO3 but not with BCi-N compared to the respective Control in both soils, which is in good agreement with the release experiments in phosphate buffer. The effect of acidification in BCi-HNO₃ on reduction of NO₃ leaching was only significantly maintained compared to the Control in soil-2.3 and not in the more alkaline soil-2.4 N during subsequent leaching events (until 2 SPV cumulative leaching), indicating that BCi-HNO₃ was faster equilibrated to environmental pH in the alkaline soil, which resulted in lower sorption of NO₃ in BCi-HNO₃. In soil-2.3, BCi-HNO₃ reduced NO₃ leaching compared to the Control more significant as BCi-N after re-fertilization, indicating that biochar acidification still improved NO₃ sorption to biochar even 12 days after application to soil. In soil-2.4 N, this effect did not occur, i.e., the initially higher NO₃ sorption capacity of BCi-HNO₃ was lost. This synchronization effect of BCi-N and BCi-HNO₃ in terms of the NO₃ leaching is the result of biochar equilibration to soil pH, which increases the NO₃ sorption capacity for BCi-N (initial bulk pH of 9) and decreases sorption capacity of BCi-HNO₃ (initial bulk pH = 5.4). Equilibration of BCi-N to environmental pH might take longer in the soil with lower pH than at higher pH, leading to a longer maintained difference to BCi-HNO3 in soil-2.3 N. At the same time, BCi-HNO₃ was already nearly at the same pH as soil-2.3 (= pH 5.7) and therefore maintained its initial NO₃ sorption ability, while in soil-2.4 N, BCi-HNO₃ lost sorption capacity due to equilibration to higher pH, explaining the faster synchronization with BCi-N.

The soils not only differed in pH but also in texture, which might have affected the general potential of the biochar application on NO_3^- leaching reduction (Borchard et al., 2019), but likely not the differences observed between BCi-N and BCi-HNO $_3$ compared to the Control. Furthermore, the timing of the first leaching event after BBF application to soil (four days in the present study) and soil moisture content might be crucial for the extent of NO_3^- leaching reduction through the acidification treatment, as it affects pH equilibration to soil conditions. The

timing of the first leaching event was, however, not an experimental factor in the present study. Further, the soil moisture was adjusted to 65 % WHC on the initial three days after column setup. After the first leaching event, the soil was water saturated for the whole experiment, since a leaching event was conducted each day, and thus, soil moisture is not likely to have been a limiting factor for pH equilibration.

The leaching experiments were only performed with BCi due to a sample shortage of the biochars produced at pilot-plant scale. Higher reductions in NO_3^- leaching compared to the Control might have been achieved with BC750 and BC900 in both soils, as NO_3^- sorption to these biochars was higher in batch sorption experiments compared to BCi. The industrial biochar used here was produced at a moderate 650 °C, while there are also several industrial biochar production plants in operation that can use HTT of up to 900 °C. Ultimately, it must be mentioned that the small-scaled column leaching experiments can only reflect effects on NO_3^- leaching induced by physico-chemical soil-biochar interactions related to e.g., soil texture and pH, however, processes such as preferential flow, soil surface runoff or bioturbation are not covered.

4.4. Biochar modification to improve NO₃ sorption

This study focused on modifying biochar with acid to improve its NO₃ sorption capacity and potential to reduce NO₃ leaching. Other modification techniques of biochar in this context include steam activation to increase available SSA of biochar (Borchard et al., 2012) or metal-enrichment of biomass prior to pyrolysis with e.g., lanthanum, potassium, or magnesium oxides to increase the number of anion sorption sites in biochar (Dieguez-Alonso et al., 2019; Wang et al., 2015; Zhang et al., 2012). Compared to acidification, the effects obtained from these methods might last longer after biochar soil application, as the effects of acidification may fade more quickly due to equilibration with environmental pH. However, steam activation will considerably decrease biochar yield by 30-70 % (Hagemann et al., 2020). Metal-enrichment, in contrast, may increase biochar yield (Grafmüller et al., 2022; Mašek et al., 2019), but to the best of our knowledge, optimizing both carbon yield and nitrate sorption capacity simultaneously has not been studied yet. Still, adding N as HNO3 to biochar could be a cost-effective strategy to enhance its initial NO3 sorption capacity, as the cost of N added via HNO3 or KNO3 is comparable (approximately 7 € (kg N)⁻¹, (Chemieshop24, 2025; Duengerexperte, 2025) and it can be implemented without modification of the pyrolysis process. Biochar acidification represents a tool to improve the short-term interaction of biochar with NO₃ spiked into its pores during BBF production, independent of any pre-pyrolysis treatment of the biochar feedstock. To increase the effect of biochar acidification on increases in NO₃ sorption capacity, physical activation could be considered based on the present study but also a maximization of aromaticity by choosing a high HTT during pyrolysis or increasing graphitization by using pyrolysis additives, such as isopropanol (Fornari et al., 2025).

4.5. Implications for practical biochar application in agriculture

The results of this study highlight the advantage of using biochar produced at a HTT $>750~{\rm C}$ to increase NO_3^- sorption and thus improve the retention of NO_3^- in biochar amended soils. Based on release experiments in aqueous suspension and in soil columns, biochar acidification has the potential to improve the slow-release of NO_3^- from biochar-based fertilizers. This, however, needs to be studied in follow up experiments under field conditions to evaluate the practical relevance of the proposed treatment, also taking into account the risk of soil acidification under the proposed treatment. Such experiments would include effects such as preferential flow, surface runoff, or bioturbation, which can influence NO_3^- leaching. Our results can support scientists and practitioners by developing new formulations of biochar-based fertilizers for such field experiments.

5. Conclusions

The findings of this study suggest, in line with our hypothesis, that the dominant mechanism of pH-dependent NO₃ sorption to biochar is related to sorption to protonated aromatic structures, especially for biochar produced at HTT >500 °C. Nitrate sorption to biochar and thus, biochar's potential to reduce NO3 leaching increases as soil pH decreases and can be maximized by conducting pyrolysis at > 750 °C. With biochar repeatedly applied over several years and ultimately accumulating to 5-10 t ha-1, which is considered the optimistic economic break-even point reached after 10 years (Bach et al., 2016), 30-60 kg N ha⁻¹ can maximally be sorbed and prevented from rapid leaching in slightly acidic soils and 10–25 kg N ha⁻¹ in pH-neutral soils, which is of agricultural relevance. Acidification of biochar with HNO₃ can be a cost-neutral option for production of biochar-based fertilizers to reduce NO₃ leaching instantly after biochar application to soil. Still, a long-term effect of the acidification treatment on NO₃ leaching is unlikely due to biochar's equilibration to environmental pH. Thus, the relevance of this biochar treatment needs to be evaluated under field conditions. The focus of the present study was to investigate and enhance the sorption of NO₃ to pristine biochar as it is the prevailing N species present in soils. To produce a BBF, however, also other mineral or organic N sources, which potentially have higher sorption affinity to pristine biochars compared to NO3, like urea, should be considered to provide N-enriched biochars with optimal slow-release fertilization properties.

CRediT authorship contribution statement

Jannis Grafmüller: Writing – original draft, Investigation, Conceptualization. Hans-Peter Schmidt: Writing – review & editing, Supervision. Daniel Kray: Writing – review & editing, Supervision, Funding acquisition. Thomas D. Bucheli: Writing – review & editing, Conceptualization. Haike Mäurer: Writing – review & editing, Investigation. Jens Möllmer: Writing – review & editing, Investigation. Heiko Peisert: Writing – review & editing, Resources, Formal analysis. Nikolas Hagemann: Writing – review & editing, Supervision, Conceptualization.

Declaration of competing interest

The authors declare the following financial interests/personal relationships which may be considered as potential competing interests: Hans-Peter Schmidt and Nikolas Hagemann reports a relationship with Carbon Standards International AG that includes: board membership. If there are other authors, they declare that they have no known competing financial interests or personal relationships that could have appeared to influence the work reported in this paper.

Acknowledgments

This research was conducted within the HyPErFarm project (htt ps://hyperfarm.eu/), which has received funding from the European Union's Horizon 2020 research and innovation programme under grant agreement no. 101000828. Syed Mustafa Hussain and colleagues at University of Tuebingen are acknowledged for the assistance during XPS measurements. Christian Gramlich from AWN GmbH is acknowledged for the provision of BCi, the industrially produced biochar. Rivka Fidel is acknowledged for valuable feedback on the methodology of the Boehm titration for acidic groups. We thank all the staff of the analytical chemistry lab at Offenburg University for assistance and provision of lab space and equipment, especially Andrea Seigel, Regina Brämer and Barbara Anders.

Appendix A. Supplementary data

Supplementary data to this article can be found online at https://doi.org/10.1016/j.jenvman.2025.127224.

Data availability

Data will be made available on request.

References

- Bach, M., Wilske, B., Breuer, L., 2016. Current economic obstacles to biochar use in agriculture and climate change mitigation. Carbon Manag. 7, 183–190. https://doi. org/10.1080/17583004.2016.1213608
- Banik, C., Lawrinenko, M., Bakshi, S., Laird, D.A., 2018. Impact of pyrolysis temperature and feedstock on surface Charge and Functional Group chemistry of biochars. J. Environ. Qual. 47, 452–461. https://doi.org/10.2134/jeq2017.11.0432.
- Bartolomei, M., Hernández, M.I., Campos-Martínez, J., Hernández-Lamoneda, R., 2019. Graphene multi-protonation: a cooperative mechanism for proton permeation. Carbon 144, 724–730. https://doi.org/10.1016/j.carbon.2018.12.086.
- Boehm, H.P., 2001. Carbon surface chemistry. In: Graphite and Precursors, vol. 1. Gordon and Breach Science Publishers, pp. 141–178.
- Boehm, H.P., 1994. Some aspects of the surface chemistry of carbon blacks and other carbons. Carbon 32, 759–769. https://doi.org/10.1016/0008-6223(94)90031-0.
- Borchard, N., Schirrmann, M., Cayuela, M.L., Kammann, C., Wrage-Mönnig, N., Estavillo, J.M., Fuertes-Mendizábal, T., Sigua, G., Spokas, K., Ippolito, J.A., Novak, J., 2019. Biochar, soil and land-use interactions that reduce nitrate leaching and N2O emissions: a meta-analysis. Sci. Total Environ. 651, 2354–2364. https://doi.org/10.1016/j.scitotenv.2018.10.060.
- Borchard, N., Wolf, A., Laabs, V., Aeckersberg, R., Scherer, H.W., Moeller, A., Amelung, W., 2012. Physical activation of biochar and its meaning for soil fertility and nutrient leaching - a greenhouse experiment: physical activation of biochar. Soil Use Manag. 28, 177–184. https://doi.org/10.1111/j.1475-2743.2012.00407.x.
- Chemieshop 24, 2025. Salpetersäure 53% techn, 1200 kg Container) [WWW Document]. Salpetersäure 53% techn. (1200kg Container). URL. https://www.chemieshop 24. de/salpetersaeure-53-techn.-1200kg-container/1000409201002. (Accessed 7 July 2025).
- Chia, 2015. Characteristics of biochar: physical and structural properties. In: Lehmann, J., Joseph, S. (Eds.), Biochar for Environmental Management: Science, Technology and Implementation. Routledge, Taylor & Francis Group, London; New York. https://doi.org/10.4324/9780203762264-12.
- Chintala, R., Mollinedo, J., Schumacher, T.E., Papiernik, S.K., Malo, D.D., Clay, D.E., Kumar, S., Gulbrandson, D.W., 2013. Nitrate sorption and desorption in biochars from fast pyrolysis. Microporous Mesoporous Mater. 179, 250–257. https://doi.org/ 10.1016/j.micromeso.2013.05.023.
- Conte, P., Schmidt, H.-P., 2017. Soil-Water interactions unveiled by fast field cycling NMR relaxometry. In: Harris, R.K., Wasylishen, R.L. (Eds.), Emagres. John Wiley & Sons, Ltd, Chichester, UK, pp. 453–464. https://doi.org/10.1002/9780470034590. emrstm1535.
- Dieguez-Alonso, A., Anca-Couce, A., Frišták, V., Moreno-Jiménez, E., Bacher, M., Bucheli, T.D., Cimò, G., Conte, P., Hagemann, N., Haller, A., Hilber, I., Husson, O., Kammann, C.I., Kienzl, N., Leifeld, J., Rosenau, T., Soja, G., Schmidt, H.-P., 2019. Designing biochar properties through the blending of biomass feedstock with metals: impact on oxyanions adsorption behavior. Chemosphere 214, 743–753. https://doi. org/10.1016/j.chemosphere.2018.09.091.
- Duengerexperte, de, 2025. Kaliumnitrat Multi-K RECI 13,5 0 46,5 [WWW Document]. Kaliumnitrat Multi-K RECI 13,5 0 46,5. URL. https://www.duengerexperte.de/de/Kaliumnitrat.html. (Accessed 7 July 2025).
- EBC 2012-2024, 2024. European Biochar Certificate guidelines for a sustainable production of biochar. Carbon Standards International (CSI), Frick, Switzerland. 10 (4). http://european-biochar.org. from 20th Dec 2024.
 Fidel, R.B., Laird, D.A., Spokas, K.A., 2018. Sorption of ammonium and nitrate to
- Fidel, R.B., Laird, D.A., Spokas, K.A., 2018. Sorption of ammonium and nitrate to biochars is electrostatic and pH-dependent. Sci. Rep. 8, 17627. https://doi.org/ 10.1038/s41598-018-35534-w.
- Fidel, R.B., Laird, D.A., Thompson, M.L., 2013. Evaluation of modified boehm titration methods for use with biochars. J. Environ. Qual. 42, 1771–1778. https://doi.org/ 10.2134/jeq2013.07.0285.
- Fornari, M.R., Hryniewicz, B.M., Matos, T.T.S., Schultz, J., Vidotti, M., Mangrich, A.S., 2025. Graphene-like biochars from pyrolysis of sugarcane bagasse and exhausted black acacia bark for the production of supercapacitors. Biomass Bioenergy 193, 107567. https://doi.org/10.1016/j.biombioe.2024.107567.
- Gai, X., Wang, H., Liu, J., Zhai, L., Liu, S., Ren, T., Liu, H., 2014. Effects of feedstock and pyrolysis temperature on biochar adsorption of ammonium and nitrate. PLoS One 9, e113888. https://doi.org/10.1371/journal.pone.0113888.
- Gezahegn, S., Sain, M., Thomas, S., 2019. Variation in feedstock wood chemistry strongly influences biochar liming potential. Soil Syst. 3, 26. https://doi.org/10.3390/ soilsystems3020026.
- Grafmüller, J., Böhm, A., Zhuang, Y., Spahr, S., Müller, P., Otto, T.N., Bucheli, T.D., Leifeld, J., Giger, R., Tobler, M., Schmidt, H.-P., Dahmen, N., Hagemann, N., 2022. Wood ash as an additive in biomass pyrolysis: effects on biochar yield, properties, and agricultural performance. ACS Sustain. Chem. Eng. 10, 2720–2729. https://doi. org/10.1021/acssuschemeng.1c07694.

- Hagemann, N., Joseph, S., Schmidt, H.-P., Kammann, C.I., Harter, J., Borch, T., Young, R. B., Varga, K., Taherymoosavi, S., Elliott, K.W., McKenna, A., Albu, M., Mayrhofer, C., Obst, M., Conte, P., Dieguez-Alonso, A., Orsetti, S., Subdiaga, E., Behrens, S., Kappler, A., 2017. Organic coating on biochar explains its nutrient retention and stimulation of soil fertility. Nat. Commun. 8, 1089. https://doi.org/10.1038/s41467-017-01123-0.
- Hagemann, N., Schmidt, H.-P., Kägi, R., Böhler, M., Sigmund, G., Maccagnan, A., McArdell, C.S., Bucheli, T.D., 2020. Wood-based activated biochar to eliminate organic micropollutants from biologically treated wastewater. Sci. Total Environ. 730. https://doi.org/10.1016/j.scitotenv.2020.138417.
- Haider, G., Joseph, S., Steffens, D., Müller, C., Taherymoosavi, S., Mitchell, D., Kammann, C.I., 2020. Mineral nitrogen captured in field-aged biochar is plantavailable. Sci. Rep. 10. https://doi.org/10.1038/s41598-020-70586-x, 13816.
- Heaney, N., Ukpong, E., Lin, C., 2020. Low-molecular-weight organic acids enable biochar to immobilize nitrate. Chemosphere 240, 124872. https://doi.org/10.1016/ ichemosphere 2019 124872
- Hood-Nowotny, R., Umana, N.H.-N., Inselbacher, E., Oswald- Lachouani, P., Wanek, W., 2010. Alternative methods for measuring inorganic, organic, and total dissolved nitrogen in soil. Soil Sci. Soc. Am. J. 74, 1018–1027. https://doi.org/10.2136/ ssssi2000.0389
- Ippolito, J.A., Cui, L., Kammann, C., Wrage-Mönnig, N., Estavillo, J.M., Fuertes-Mendizabal, T., Cayuela, M.L., Sigua, G., Novak, J., Spokas, K., Borchard, N., 2020. Feedstock choice, pyrolysis temperature and type influence biochar characteristics: a comprehensive meta-data analysis review. Biochar. https://doi.org/10.1007/s42773-020-00067-x.
- Issi, J.-P., 2001. Electronic conduction. In: Graphite and Precursors, vol. 1. Gordon and Breach Science Publishers, pp. 45–70.
- Kopp, C., Sica, P., Lu, C., Tobler, D., Stoumann Jensen, L., Müller-Stöver, D., 2023. Increasing phosphorus plant availability from P-rich ashes and biochars by acidification with sulfuric acid. J. Environ. Chem. Eng. 11, 111489. https://doi.org/ 10.1016/j.jece.2023.111489.
- Lawrinenko, M., Laird, D.A., 2015. Anion exchange capacity of biochar. Green Chem. 17, 4628–4636. https://doi.org/10.1039/C5GC00828J.

- Lehmann, J., Joseph, S. (Eds.), 2015. Biochar for Environmental Management: Science, Technology and Implementation, second ed. Routledge, Taylor & Francis Group, London; New York.
- Mašek, O., Buss, W., Brownsort, P., Rovere, M., Tagliaferro, A., Zhao, L., Cao, X., Xu, G., 2019. Potassium doping increases biochar carbon sequestration potential by 45%, facilitating decoupling of carbon sequestration from soil improvement. Sci. Rep. 9, 5514. https://doi.org/10.1038/s41598-019-41953-0.
- Melo, L.C.A., Lehmann, J., Carneiro, J.S. da S., Camps-Arbestain, M., 2022. Biocharbased fertilizer effects on crop productivity: a meta-analysis. Plant Soil. https://doi.org/10.1007/s11104-021-05276-2.
- Mochidzuki, K., Soutric, F., Tadokoro, K., Antal, M.J., Tóth, M., Zelei, B., Várhegyi, G., 2003. Electrical and physical properties of carbonized charcoals. Ind. Eng. Chem. Res. 42, 5140–5151. https://doi.org/10.1021/ie030358e.
- Nightingale, E.R., 1959. Phenomenological theory of ion solvation. Effective radii of hydrated ions. J. Phys. Chem. 63, 1381–1387. https://doi.org/10.1021/ i150570a011
- PYREG, 2025. P1500 biomasse [WWW Document]. URL. https://www.pyreg.de/p1-500-biomasse/.
- Schubert, S., 2018. Pflanzenernährung, 3. In: Auflage, vollständig überarb (Ed.), UTB Agrarwissenschaften. Verlag Eugen Ulmer, Stuttgart.
- Singh, B., Camps-Arbestain, M., Lehmann, J., 2017. CSIRO (Australia). Biochar: a Guide to Analytical Methods. CSIRO Publishing, Clayton, Victoria.
- Wang, Z., Guo, H., Shen, F., Yang, G., Zhang, Y., Zeng, Y., Wang, L., Xiao, H., Deng, S., 2015. Biochar produced from oak sawdust by Lanthanum (La)-involved pyrolysis for adsorption of ammonium (NH4+), nitrate (NO3-), and phosphate (PO43-). Chemosphere 119, 646-653. https://doi.org/10.1016/j.chemosphere.2014.07.084.
- Yang, J., Li, H., Zhang, D., Wu, M., Pan, B., 2017. Limited role of biochars in nitrogen fixation through nitrate adsorption. Sci. Total Environ. 592, 758–765. https://doi. org/10.1016/j.scitotenv.2016.10.182.
- Zhang, M., Gao, B., Yao, Y., Xue, Y., Inyang, M., 2012. Synthesis of porous MgO-biochar nanocomposites for removal of phosphate and nitrate from aqueous solutions. Chem. Eng. J. 210, 26–32. https://doi.org/10.1016/j.cej.2012.08.052.